

# An ORMOSIL porous double-layer broadband antireflective coating

Huai Xiong (熊怀)<sup>1,2,\*</sup>, Yongxing Tang (唐永兴)<sup>1</sup>, Lili Hu (胡丽丽)<sup>3</sup>,  
and Haiyuan Li (李海元)<sup>1</sup>

<sup>1</sup>Key Laboratory of High Power Laser and Physics, Shanghai Institute of Optics and Fine Mechanics, Chinese Academy of Sciences, Shanghai 201800, China

<sup>2</sup>University of Chinese Academy of Sciences, Beijing 100049, China

<sup>3</sup>Key Laboratory of Materials for High Power Laser, Shanghai Institute of Optics and Fine Mechanics, Chinese Academy of Sciences, Shanghai 201800, China

\*Corresponding author: xhuai1998@siom.ac.cn

Received November 9, 2018; accepted December 14, 2018; posted online March 1, 2019

A  $\lambda/4$ - $\lambda/4$  broadband antireflective (AR) coating is developed with a sol-gel dip-coating method. By adding SAR-5 organosilicon resin into a base-catalyzed silica sol top layer and treating at 300°C, a broadband AR coating used for blast shields with a high average transmission of 99.34% (450–950 nm) and good hydrophobicity (with a water-contact angle of 119°) was obtained. After being subjected to rubbing 50 times and being maintained at a relative humidity of around 95% for 50 days, the average transmission of the coating decreased by 0.29% and 0.04%, respectively. This indicates that the organically modified silica (ORMOSIL) broadband AR coating has good abrasion resistance and humidity stability.

OCIS codes: 310.1210, 160.6060, 310.4165, 240.0310.

doi: 10.3788/COL201917.033101.

The sol-gel method is the most commonly used method that is employed to obtain antireflective (AR) films, and it possesses excellent stability, reproducibility, and low production costs; this method is also used to fabricate silica optical fibers<sup>[1–5]</sup>. These AR coatings have high damage thresholds that are 2–3 times that of other coating materials, which is a requirement for high-power laser systems. They are widely used as coatings on amplifier windows, quartz glass windows, and harmonic converter crystals<sup>[6]</sup>. Research into the quarter-wave single-layer AR coating is a popular topic in the AR field, and it has widespread application in high-power laser systems. With these single-layer coatings, the optimal efficiency is suitable for one wavelength<sup>[7]</sup>. However, there are many other situations in which a broader-band coating is required. Obvious examples are harmonic converter crystals, solar cover glass, display systems, and blast shields<sup>[7–14]</sup>.

In high-power laser systems, blast shields separate the flashlamps from the glass laser slabs to prevent damage to expensive amplifiers due to potential explosions<sup>[15,16]</sup>. Considering the difficulty in controlling the coating thickness, double-layer films are widely used, and the typical design includes  $\lambda/4$ - $\lambda/2$  type and  $\lambda/4$ - $\lambda/4$  type (where  $\lambda$  is the center wavelength) films. Thomas<sup>[2]</sup> developed a simple two-layer broadband coating that consists of a layer of a methyl silicone polymer overcoated with porous silica. With this approach, less than 0.5% reflection can be achieved over a 500–1100 nm wavelength range. However, the top porous silica layer has weak mechanical properties, which limits its application. Zhang *et al.*<sup>[13]</sup> designed a double-layer double-wavelength AR coating with 100%

transmittance at both 1064 and 532 nm, which is very important in high-power laser systems, and the coating was designed using thin-film design software. The sol-gel process consists of a good experimental method that achieves this design. Prené *et al.*<sup>[11]</sup> designed and developed a type of  $\lambda/4$ - $\lambda/2$  SiO<sub>2</sub>/Ta<sub>2</sub>O<sub>5</sub> broadband AR coating that has an expected amplification gain of close to 6%; however, the transmittance at the center wavelength was relatively low (less than 97%). Jia *et al.*<sup>[17]</sup> reported a  $\lambda/4$ - $\lambda/2$  SiO<sub>2</sub>/TiO<sub>2</sub> AR coating used in amplifier blast shields of the Shengguang-II (SG-II) facility. The average transmission of dual-coated K9 substrates was increased by 6.6% compared to uncoated substrates in the spectral range 400–700 nm. However, the optical properties of such  $\lambda/4$ - $\lambda/2$  type coatings need to be improved. Compared with the  $\lambda/4$ - $\lambda/2$  design,  $\lambda/4$ - $\lambda/4$  broadband AR coatings feature a flat broadband transmission spectrum. Li *et al.*<sup>[12]</sup> utilized a  $\lambda/4$ - $\lambda/4$  wavelength system, achieving an average transmittance for coated borosilicate crown (BK7) glass of more than 99.5% over the range of 500–850 nm. NH<sub>3</sub> heat and trimethylchlorosilane treatment enhance the scratch resistance and moisture resistance of these coatings.

In this work, a  $\lambda/4$ - $\lambda/4$  organically modified silica (ORMOSIL) porous broadband AR coating, which has moisture resistance and abrasion resistance, was developed by using a modified top layer with SAR-5 resin (SAR-5, wear-resisting methyl silicone resin binder that can increase the wear-resistance and hydrophobicity properties of coating after heat treatment)<sup>[18]</sup>. This coating exhibits a flat broadband transmission spectrum from 450 to 950 nm. The abrasion resistance and humidity stability

were measured and compared to coatings without methyl silicon resin.

Base-catalyzed silica sol was prepared by mixing tetraethoxysilane (TEOS),  $H_2O$ ,  $NH_3$ , and anhydrous ethanol ( $C_2H_5OH$ ) in the molar ratio 1:2:0.9:34.2, respectively<sup>[3]</sup>, and this is marked as Z1. The chemical reagents were stirred vigorously for more than 5 h at about 5°C. After stirring for 2 h at 20°C, all of the solutions were placed into an oven to age for 7 days at 60°C. Finally, the solutions needed to be refluxed to remove ammonia. SAR1-Z, SAR3-Z, and SAR5-Z sols (adding 5% volume *n*-propanol) were synthesized with mixed sols; the SAR-5:Z1 sol volume ratios were 1:100, 3:100, and 5:100, respectively. Acid-catalyzed sol was synthesized by mixing TEOS,  $H_2O$ , hydrochloric acid (HCl), and  $C_2H_5OH$  in the molar ratio 1:4:0.01:20; this solution was ready for use after being stirred for 4 h and aged for at least 4 days at room temperature. BC1 sol was prepared by mixing 120 mL B sol (TEOS,  $H_2O$ ,  $NH_3$ , and  $C_2H_5OH$  in the molar ratio 1:2.9:0.49:34.2, respectively, where the chemical reagents were stirred vigorously for more than 5 h at 20°C, then at least 6 days at 60°C, and finally ammonia was removed), 63 mL acid-catalyzed sol, and 10 mL *n*-propanol (suitable adjustments to the B sol and acid-catalyzed sol proportion can be made according to the deviation from the required refractive index). For the double-layer coating preparation, bottom layers were prepared by using a dip-coating process with BC1 sol on the fused silica glass. The prepared coatings were heated at 200°C for 10 min. Subsequently, top layers were prepared by dip-coating with Z1, SAR1-Z, SAR3-Z, and SAR5-Z sols, respectively, to finally obtain the double-layer broadband AR coatings BCZ1, BCSAR1, BCSAR3, and BCSAR5, respectively. The coatings were put into an oven again at 200°C or 300°C for 10–30 min.

Transmission spectra of coatings prepared with SAR1-Z, SAR3-Z, SAR5-Z, and BC1 sols were measured with a spectrophotometer (Perkin-Elmer Lambda 900, 150 mm integrating sphere), and the refractive indices of  $SiO_2$  AR coatings were measured with a HORIBA UVI-SEL 2 and Sopra GES-5 E spectroscopic ellipsometer, the results of which are shown in Fig. 1. The peak transmission of SAR1-Z was above 99.9%, showing almost no change after treatment at 200°C or 300°C, with a refractive index of 1.20 at a wavelength of 650 nm after treatment at 300°C. Correspondingly, the peak transmission of SAR3-Z increased from 99.87% to above 99.99% (200°C) and above 99.99% (300°C), with a refractive index of 1.22 at a wavelength of 650 nm after treatment at 300°C. The peak transmission of SAR5-Z clearly increased from 99.36% to 99.76% (200°C) and 99.80% (300°C,  $n = 1.25$ , 650 nm). Figure 1(d) shows the transmission spectra of the BC1 coating after treatment at 200°C. The refractive index of the BC1 coating was estimated to be around 1.37 according to the peak transmission (96.95%), which is consistent with the theoretical design value of thin-film design software TFCalc. (With the storage of BC sol for several hours, the refractive index of the film will increase slowly.

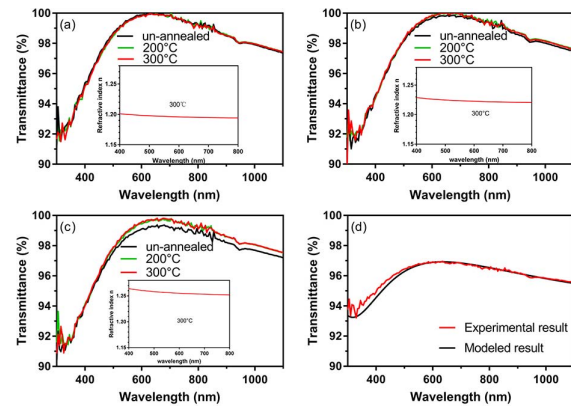


Fig. 1. Transmission spectra of the (a) SAR1-Z coating, (b) SAR3-Z coating, (c) SAR5-Z coating, and (d) BC1 coating.

It is necessary to select the appropriate time to obtain the required coating refractive index.) It can be seen that as the increment of SAR-5 resin grows, the transmission of the coating declines at a faster rate. Furthermore, the increase of the treatment temperature contributed to an increase in the coating peak transmission. Figure 2 shows the water-contact angle (measured using a DataPhysics OCA40 instrument) of the different coatings and the thermogravimetry (TG) differential scanning calorimetry (DSC, METTLER TOLEDO TGA/DSC1/1600HT) curves obtained in  $O_2$  atmosphere for the SAR3-Z gel. A weight loss of 10% is shown in the TG curves in the temperature range 30°C–237°C, and this is attributed to the evaporation of water and organic solvents. Two exothermic peaks at around 325°C and 497°C are attributed to the condensation between Si-OH and the oxidation of Si- $CH_3$  to Si-OH, respectively<sup>[19]</sup>. This resulted in a gradual increase in the peak transmission of SAR3-Z and SAR5-Z coatings after treatment at 200°C and 300°C, as shown in Fig. 1. For the SAR1-Z, SAR3-Z, and SAR5-Z coatings, the water-contact angles were 121°, 118°, and 119°, respectively, with good hydrophobicity owing to the Si- $CH_3$  hydrophobic groups of the SAR-5 resin. As the heat-treatment temperature increased to 200°C, all three water-contact angles increased by 3°–6°, owing to the evaporation of water and organic solvents. However, the water-contact angle of coatings after treatment at 300°C decreased by 12°, 5°, and 4°, respectively, compared with treatment at 200°C. The loss of the water-contact angle should be attributed to the transformation of hydrophobic Si- $OC_2H_5$  into hydrophilic Si-OH in the coating

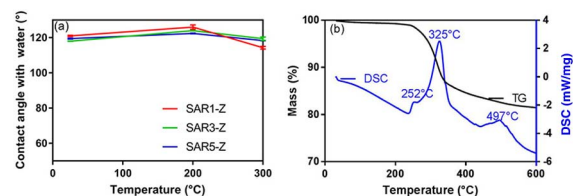


Fig. 2. (a) Water-contact angle of the SAR1-Z, SAR3-Z, and SAR5-Z coating and (b) TG-DSC curve for the SAR3-Z gel.

under treatment, which can be confirmed by a slight exothermic peak at 252°C in the TG-DSC analysis. In comparison, the lower amount of SAR-5 resin with hydrophobic methyl groups in SAR1-Z resulted in a greater decrease in the water-contact angle compared with SAR3-Z and SAR5-Z. A treatment temperature of 300°C was selected for the coatings based on the following considerations: (1) the increase in the coating peak transmission and good hydrophobicity after treatment at 300°C; (2) oven heating (from room temperature to 300°C) is suitable for larger-size optic elements; and (3) heat treatment above 300°C may affect the surface shape of optical glass.

Figure 3 shows the transmission spectra for the double-layer broadband porous silica AR coatings, as well as the theoretical transmission spectrum of the double-layer broadband AR coating, which is calculated by TFCalc. The average transmission of the BCZ1 coating after 300°C (in the spectral range of 450–950 nm) decreased slightly from 99.52% to 99.45% after NH<sub>3</sub> heat treatment (20 mL NH<sub>3</sub> · H<sub>2</sub>O, 150°C/24 h) and had excellent optical properties. The  $\lambda/4$ - $\lambda/4$  system and a central wavelength of 640 nm were chosen for the simulation. Because the refractive indices of BCSAR1, BCSAR3, and BCSAR5 coatings were 1.20, 1.22, and 1.25, respectively, different indices of the bottom layer were used to calculate the theoretical transmission spectrum. We chose the BC1 coating with a refractive index of 1.37 as

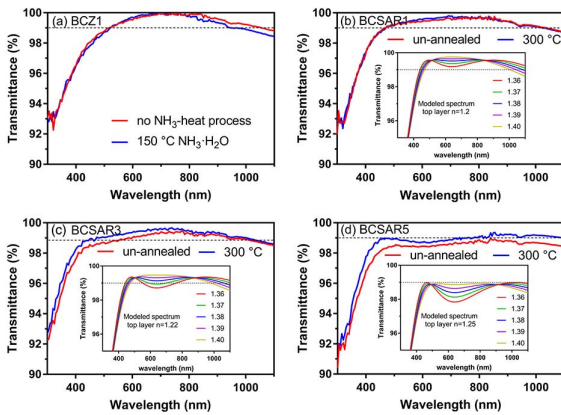


Fig. 3. Transmission spectra of the (a) BCZ1, (b) BCSAR1, (c) BCSAR3, and (d) BCSAR5 coatings.

the bottom layer, which should perform well for broadband AR applications, and the thicknesses ( $d$ ) of the bottom layer were around 117 nm, which correspond to the optical thickness ( $nd = \lambda/4$ ). The thicknesses of the top layer were around 133 nm (SAR1-Z), 131 nm (SAR3-Z), and 128 nm (SAR5-Z). The experimental transmittance spectrum has some small deviations compared with that of the modeled spectrum, and this may be caused by the deviation in the thickness of two layers from the model or the interface penetration between two layers. Before and after annealing at 300°C, the average transmittance of BCSAR1, BCSAR3, and BCSAR5 increased from 99.45% to 99.49%, 99.08% to 99.34%, and 98.56% to 98.95%, respectively. It was demonstrated that the increase for SAR-5 resin led to an accelerated degeneration of the coating transmission. Because of the poor transmission performance, the BCSAR5 coating is not suitable as a broadband AR coating. Therefore, BCSAR1 and BCSAR3 coatings are the focus of the following discussion.

Regarding the practical use of these broadband AR coatings for blast shields, their abrasion resistance is a key consideration. The abrasion resistance test was carried out by rubbing the coatings with a micro denier wiper (instead of cotton ball) immersed in ethanol<sup>[12]</sup>. Table 1 lists the measured average transmission (450–950 nm) before and after different rubbing times. The NH<sub>3</sub>-treated BCZ1 coating could be removed after five rubbings. The decrease in the average transmission of the BCSARZ1 (200°C) coating was more serious than for the NH<sub>3</sub>-treated BCZ1 coating, while there was an enhanced abrasion resistance after treatment at 300°C. This enhanced abrasion resistance was more pronounced for the BCSARZ3 (300°C) coating, for which the average transmittance only decreased by 0.29% after rubbing 50 times; this is equivalent to the average transmittance decrease of the BCSARZ3 (200°C) coating after rubbing 3–5 times. After treatment at 300°C, the use of SAR-5 resin as a binder served to increase the adhesion between individual silica particles by Si-OH condensation, which is consistent with the exothermic peak observed in the TG-DSC data at around 325°C. This increased the coating strength.

Another critical property for amplifier blast shields is the humidity stability of coatings. This is because the adsorption of water leads to a reduction in the optical

Table 1. Transmission of the Coatings Before and After Abrasive Rubbing

Coating	Average Transmittance (%)	Average Transmittance Reduction After Rubbing (%)					
		1 time	3 times	5 times	10 times	20 times	50 times
BCZ1 NH <sub>3</sub>	99.28	0.96	1.50	2.24	/	/	/
BCSAR1 200°C	99.49	1.48	1.58	/	/	/	/
BCSAR1 300°C	99.50	0.36	0.94	1.73	/	/	/
BCSAR3 200°C	99.34	0.17	0.21	0.41	1.00	1.67	/
BCSAR3 300°C	99.33	0.01	0.01	0.03	0.08	0.07	0.29

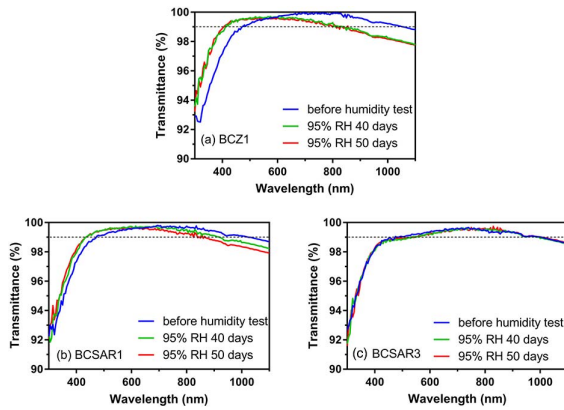


Fig. 4. Transmission of the broadband AR coatings (a) BCZ1, (b) BCSAR1, and (c) BCSAR3 before and after exposure to 95% RH.

transmission and, consequently, a decline in the amplification gain. The humidity stability of the coatings that can be deduced from transmission spectra was experimentally assessed by placing coating samples in a glass container in which the relative humidity (RH) was maintained at 95%–98% (defined as 95%). As shown in Fig. 4, the transmission of the BCZ1 coating after 300°C without NH<sub>3</sub> treatment declined significantly under these conditions after 40 and 50 days; the average transmission decreased from 99.64% to 99.30% and 99.23%, respectively, see Fig. 4(a). The transmittance curve for the BCZ1 coating shifted towards shorter wavelengths after being exposed to a 95% RH, and the average decrease in the transmission deteriorated when incident light of a substrate, such as blast shields, contained angular light (transmission spectrum undergoes a blue shift). The transmission spectrum of BCSAR1 experienced a slight blue shift after being maintained for 40 days, and the same trend was seen after 50 days. The average transmission of BCSAR1 decreased slightly from 99.49% to 99.46% after being maintained at 95% RH for 40 days, as shown in Fig. 4(b), and it distinctly decreased by a further 0.15% after 10 more days. The transmission spectrum of the BCSAR3 coating is shown in Fig. 4(c) and indicates excellent humidity stability. The average transmission of BCSAR3 decreased slightly from 99.34% to 99.28% and 99.30% after being maintained at 95% RH for 40 and 50 days, respectively, with almost no blue shift. The excellent humidity stability of the BCSAR3 coating confirmed the success of Si-CH<sub>3</sub> hydrophobic modification by the SAR-5 resin.

In conclusion, a  $\lambda/4$ – $\lambda/4$  double-layer broadband porous silica AR coating used for blast shields was successfully prepared with an ORMOSIL porous coating as the top layer. The BCSAR3 coating exhibited excellent optical properties with a flat broadband transmission spectrum from 450 to 950 nm. By adding SAR-5 resin to the silica sol and after treatment at 300°C, the abrasion resistance of the BCSAR3 coating was significantly increased compared to the coating without methyl silicon resin treatment by a NH<sub>3</sub> heat process, and the humidity stability was improved by Si-CH<sub>3</sub> hydrophobic modification.

## References

1. I. M. Thomas, *Appl. Opt.* **25**, 1481 (1986).
2. Y. X. Tang, Y. Q. Le, W. Q. Zhang, M. H. Jiang, J. R. Sun, and X. L. Liu, *Proc. SPIE* **3175**, 137 (1998).
3. B. Shen, H. Y. Li, H. Xiong, X. Zhang, and Y. X. Tang, *Chin. Opt. Lett.* **14**, 083101 (2016).
4. T. I. Suratwala, M. L. Hanna, E. L. Miller, P. K. Whitman, I. M. Thomas, P. R. Ehrmann, R. S. Maxwell, and A. K. Burnham, *J. Non-Crystall. Solids* **316**, 349 (2003).
5. Y. Ren, Z. Qin, G. Xie, Z. Qiao, T. Hai, P. Yuan, J. Ma, L. Qian, S. Wang, C. Yu, and L. Hu, *Chin. Opt. Lett.* **16**, 020020 (2018).
6. T. Suratwala, M. L. Hanna, and P. Whitman, *J. Non-Crystall. Solids* **349**, 368 (2004).
7. I. M. Thomas, *Proc. SPIE* **3136**, 215 (1997).
8. X. Peng, Y. Zhao, Y. Wang, G. Hu, L. Yang, and J. Shao, *Chin. Opt. Lett.* **16**, 051601 (2018).
9. J. Sun, X. Cui, C. Zhang, C. Zhang, R. Ding, and Y. Xu, *J. Mater. Chem. C* **3**, 7187 (2015).
10. K. Chandra Sekhar Reddy, D. Karthik, D. Bhanupriya, K. Ganesh, M. Ramakrishna, and S. Sakthivel, *Sol. Energy Mater. Sol. Cells* **176**, 259 (2018).
11. P. Prené, J. J. Priotton, L. Beaurain, and P. Belleville, *J. Sol-Gel Sci. Technol.* **19**, 533 (2000).
12. X. Li and J. Shen, *Thin Solid Films* **519**, 6236 (2011).
13. X. X. Zhang, S. Cai, D. You, L. H. Yan, H. B. Lv, X. D. Yuan, and B. Jiang, *Adv. Funct. Mater.* **23**, 4361 (2013).
14. X. Zhang, W. Lin, J. Zheng, Y. Sun, B. Xia, L. Yan, and B. Jiang, *J. Phys. Chem. C* **122**, 596 (2018).
15. L. Hu, S. Chen, J. Tang, B. Wang, T. Meng, W. Chen, L. Wen, J. Hu, S. Li, Y. Xu, Y. Jiang, J. Zhang, and Z. Jiang, *High Power Laser Sci. Eng.* **2**, e1 (2014).
16. J. Chen, R. Y. Shao, X. Q. Cui, X. C. Guo, J. J. Liu, and H. B. Li, *Opt. Precis. Eng.* **24**, 2988 (2016).
17. Q. Jia, Y. Le, Y. Tang, and Z. Jiang, *Acta Opt. Sin.* **24**, 65 (2004).
18. Z. Xue and J. Zhang, *Shanghai Chem. Industry* **21**, 14 (1996).
19. H. Yu, X. Liang, J. Wang, M. Wang, and S. Yang, *Solid State Sci.* **48**, 155 (2015).